Thermal Radiation Hazards from Gas Pipeline Rupture Fireballs

Cowling N.[1,2,*], Phylaktou H.[2,*], Allason D.[1], Andrews G.E.[2]

[1] *GL Industrial Services UK Ltd (DNV GL), Loughborough, Leicestershire, LE11 3GR, UK*
[2] *University of Leeds, Leeds, LS2 9JT, UK*
**Corresponding author emails: nick.cowling@dnvgl.com, h.n.phylaktou@leeds.ac.uk*

ABSTRACT

Increasing world-wide demand for gas is resulting in an increased network of gas piping which poses potential hazards to the natural and man-made environment in proximity to the pipelines. In this work we report experimental measurements of the thermal radiation levels generated by fireballs from two full-scale, below-ground, natural-gas pipeline ruptures. The tests were carried out at the DNV GL's Spadeadam Test Site simulating the rupture of a 1219 mm diameter pipe carrying high pressure natural gas (at 13.4 MPa -nominal gauge pressure). The duration of the fireball and the maximum heat fluxes (as high as 70 kW/m^2 at 200 m downwind) were well predicted by current simple mathematical models when a reasonable radiative fraction of the total energy release was assumed. The empirical radiant fraction equation adopted by OGP was shown to overpredict the incident heat flux in these tests. In the second test the grass surrounding the test location was ignited and other vegetation showed significant thermal damage. To interpret such data correctly and to evaluate the hazards, to natural and man-made environments, more information is needed on the effects of short exposure times (of the order of a few seconds) to high transient heat fluxes.

KEYWORDS: Thermal radiation, fireball, gas pipeline.

INTRODUCTION

With worldwide demand for gas is set to rise until 2034 [1]. This will inevitably lead to environmental receptors being located closer to gas transmission installations and pipelines. In the 3 years from 2013 there were 60 gas pipeline releases within the EU [2, 3]. To assess the environmental risks from a pipeline release, credible scenarios need to be considered for each site which can include unignited or ignited releases the magnitude of which will depend on the size and rate of the release and the timing of ignition after the initiation of the release. Of the potential scenarios and consequences, the full-bore rupture of an onshore pipeline and a resulting fireball represents a worst-case scenario for pipeline operators.

In the event of a rupture of an onshore natural gas transmission pipeline, high pressure gas will be instantaneously released, leading to the formation of a crater. The initial phase will be highly transient, with the formation highly turbulent jet with a mushroom cap. This initial phase typically lasts 30 seconds. The gas cloud will increase in height due to the momentum of the release and the entrained air, gradually dispersing until an almost steady state plume is developed [4].

If ignited shortly after the rupture event, combustion of the turbulent gas cloud will lead to the generation of a fireball and crater fire. Whilst missile and overpressure hazards are also generated, experience has shown that from experiments by DNV GL, the hazard ranges associated with these are smaller than thermal radiation hazards [5].

Proceedings of the Ninth International Seminar on Fire and Explosion Hazards (ISFEH9), pp. 860-868
Edited by Snegirev A., Liu N.A., Tamanini F., Bradley D., Molkov V., and Chaumeix N.
Published by Saint-Petersburg Polytechnic University Press
ISBN: 978-5-7422-6498-9 DOI: 10.18720/spbpu/2/k19-131

In the case of immediate ignition, the radiant heat flux emitted will vary significantly from the combustion of a steady state release. There are a variety of simple models for estimating thermal radiation heat flux levels from gas jet fires [6, 7] i.e. the steady state fire which develops after a fireball event. Such models have been extensively validated and refined. Publicly available data on thermal radiation data from fireballs following a large scale gas pipeline ruptures with immediate ignition are limited to few sources [8, 9]. There are however, several simple correlations for the estimation of fireball diameters and durations which have been validated for BLEVE's [7]. The International Association of Oil and Gas producers (OGP) recommend the use of one these models- discussed in detail later - to predict the thermal radiation levels for fireballs from pipelines [10].

The main aim of the present work is to provide experimental measurements of the thermal radiation levels generated following the ignition of flammable gas from a full-scale, below-ground, natural-gas pipeline rupture and to understand the implications this has for current models used in assessing the environmental risks. Evidence of thermal damage to surrounding and strategically placed vegetation will also be obtained, and this will be compared to the measured radiative fluxes and used to build up a library of vegetation damage evidence that could also be useful for investigation of pipeline fireball incidents or other thermal radiation incidents.

METHODOLODGY

The fracture propagation facility at DNV GL's Spadeadam Test Site was used to accommodate the 48-inch (1219 mm) diameter test pipes. The test layout consisted of two 48-inch (1219 mm) diameter pipe reservoirs each with a length of approximately 165 m, at a nominal test pressure of 13.5. The reservoirs were spaced with a gap between the reservoir ends of approximately 130 m where the test section comprising of eleven pipe lengths could be installed. The length of the reservoir on each end of the test section was such that it simulated an infinitely long pipeline, thus enabling that gas decompression from the test section to replicate actual pipeline conditions (at an initial 13.4 MPa gauge pressure) without experiencing any pressure reflections during the fracture event. The outer end of each of the reservoirs was terminated with a dome end and fitted with connections to a 12-inch nominal bore (323 mm) diameter gas recirculation loop through full bore isolation ball valves.

The recirculation loop incorporated a set of fan units providing a circulation velocity of nominally 0.5 m s^{-1} in the 48-inch (1219 mm) diameter test pipe to ensure that a homogeneous gas mixture was achieved throughout the test rig. A heat exchanger supplied with an ethylene glycol/water mixture and circulated through two refrigeration units was used to control the temperature of the gas. To reduce any heat loss or heat gain throughout the system, the flow loop, reservoirs and test section were insulated with spray applied polyurethane foam.

The circulating loop incorporated injection points with meters to measure both the natural gas content (injection was from an LNG source) and the volume of gas in the test rig.

To prevent reservoir movement during a test, both reservoirs were installed within large concrete anchors. Four anchors were equally spaced along each reservoir to resist any bending forces applied during the test and one at each end supported by steel piles to resist axial thrust. The reservoirs were also protected at their inner ends by wire wound crack arrestors, in the event that the fracture failed to arrest within the test section.

Prior to carrying out a pneumatic test of the rig, instrument and cable locations were covered with a layer of sand padding and then backfilled with indigenous clay type soil so that the top of the test pipes was 0.9 m below ground level. A photo of the eastern end of the test section before being backfilled is shown in Fig. 1.

The test was initiated using a 1 m long explosive cutting charge in the centre of the initiation pipe. Although there was a high probability that ignition of the test gas on initiation would occur, ignition sources were also deployed at both at high and low level by firing of pyrotechnics into the area of the cloud at the same time as the test initiation.

Fig. 1. Image of the test section prior to being backfilled.

Fig. 2. Radiometer locations**.**

The thermal radiation resulting from the fracture test was measured using an array of Medtherm wide angle radiometers (total field of view of 150^{o}) distributed around the test area. In the north-south direction (nominally crosswind from the prevailing wind direction), radiometers were placed at distances of 200 m and 500 m north of the initiation point. On the east-west axis, radiometers were placed at 200 m and 500 m west of the initiation point and distances of 200 m, 500 m, 750 m and 1000 m east of the initiation point. A diagram showing the locations and nomenclature for the radiometers is shown in Fig. 2. The radiometers have a response time of 1 s and an accuracy of ±5% and were calibrated prior to testing in a black body furnace over five different heat fluxes. Each Medtherm radiometer is fitted with a calcium fluoride window that transmits light in the wavelength range 0.3 to 11.5μm and employs a Schmidt-Boelter thermopile to measure incident thermal radiation. Incident thermal radiation is absorbed at the sensor surface and transferred to an integral heat sink that remains at a temperature below that of the sensor surface. The difference in temperature between two points along the path of the heat flow from the sensor to the sink is proportional to the heat being transferred, and is, therefore, proportional to the incident thermal radiation. Medtherm radiometers have thermocouple junctions fitted at two such points. These form a differential thermoelectric circuit, providing an EMF between the two output leads which is directly proportional to the incident thermal radiation. The radiometers will be aimed at the nominal predicted centre of the fireball.

Two full scale rupture experiments have been carried out. These tests were identical in the experimental set-up with respect to the purposes of the study presented here. However, due to a malfunction of the data loggers the East and North radiometer recordings were lost in Test 2. Additionally, there were environmental differences between the tests which are summarised in the Table 1.

Table 1. Test conditions

	Date	Ambient Temp (°C)	Atmospheric Pressure (mbar)	Relative Humidity (%)	Wind direction (°)	Wind speed (m/s)
Test 1	28th March	11	967	94	295	7.6
Test 2	6th June	9.7	984	94	253	7

RESULTS AND DISCUSSION

In the first test, a peak thermal radiation level of over 70 kW/m^2 at 200 m was observed (see Fig. 3). It took 6 seconds to reach this thermal radiation level. At 750 m it took over 20 seconds for the thermal radiation level to fall below 1 kW/m^2. The fireball mushroomed from the release point and was observed to be tilted by the prevailing wind direction (295°, 7.6 m/s) as shown in 4. Thus, the peak thermal radiation level was observed on the eastern radiometer. As a peak of 35 kW/m^2 observed on the western radiometer also located 200 m from the release point, the thermal radiation field was found to be asymmetrical.

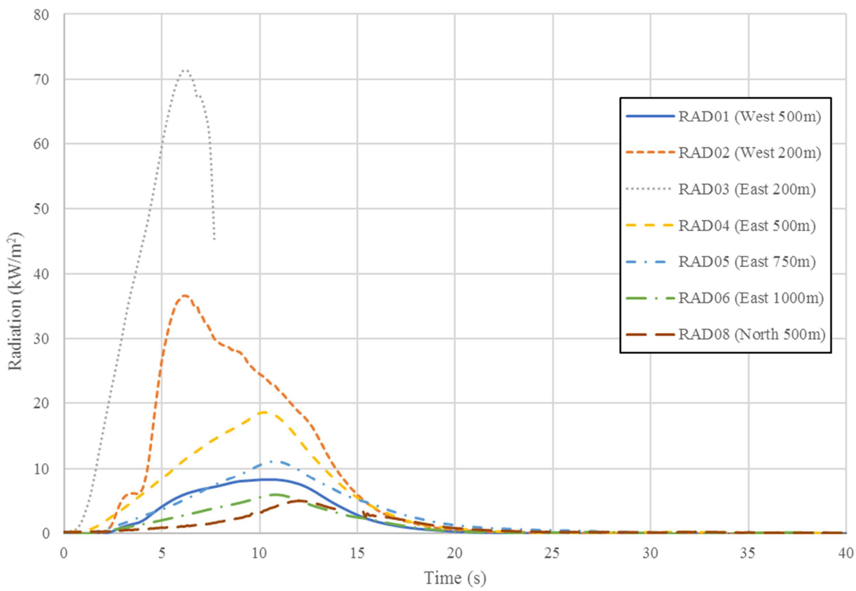

Fig. 3. Thermal Radiation Measurements from Test 1.

Comparison to calculated maximum heat fluxes

Using the same method as Wang [8], which has the same form as the OGP method [10], the peak thermal radiation at a given distance can be calculated using the equations for the maximum diameter, duration and height of the fireball:

$$D_{max} = 6.48M^{0.325} \tag{1}$$

$$H = 4.35M^{0.333} \tag{2}$$

$$t_d = 2.60M^{0.167}, \tag{3}$$

where D_{max} is the maximum diameter of the fireball (m), M the mass of fuel involved (90,000 kg), H (m) the height of the fireball from ground level and t_d (s).

The distance (X) from the fireball to the receiver is:

$$X = \sqrt{l^2 + H^2} \tag{4}$$

where l is the distance to the point on the ground beneath the fireball.

Fig. 4. Fireball from Test 1 (view looking east).

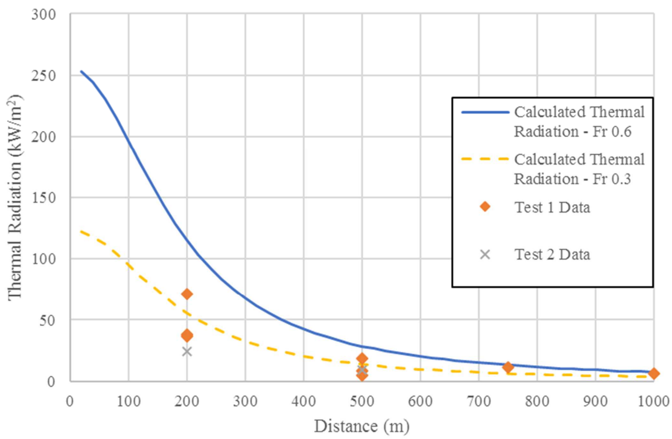

Fig. 5. Maximum thermal radiation (predicted and observed) as a function of the ground level distance from the centre of the release location.

The view factor (v_f), transmissivity (τ) and surface emissive power (E) are given by:

$$v_f = \left(\frac{D_{max}}{2X}\right)^2 \tag{5}$$

$$\tau = 2.02 \times \left[RP_w\left(X - \frac{D_{max}}{2}\right)\right]^{-0.09} \tag{6}$$

$$E = \frac{\Delta H\ M\ F_r}{\pi D_{max}^2 t_d}, \tag{7}$$

where R is the relative humidity (0.94 for Test 1), P_w is the water saturation pressure (1312 Pa) and ΔH is the heat of combustion (52 MJ/kg). The fraction of heat radiated (F_r) is given by Wang as:

$$F_r = 0.27P_b^{0.32} \tag{8}$$

where P_b is the pipe design pressure in MPa (13.4 MPa was used which is pipeline pressure before rupture) .

The radiation (I) received by an observer at distance X is:

$$I = v_f \, \tau \, E \tag{9}$$

The maximum thermal radiation levels predicted using the above model, as a function of distance from the fireball vertical axis, are shown as a solid blue line in Fig. 5, where they are compared with the measured data. Good agreement (within 20%) is shown in the far field, at distances over 700 m and low heat fluxes. In the near field the theoretical calculation overpredicts the measured values by an order of 60%.

Examination of the outputs from each of the above equations indicates that the main source of the difference is the larger than expected radiative fraction (Fr) calculated from Equation (8). The equation gives a value of Fr of 0.61 which is much larger than a generic value of 0.3 for large hydrocarbon fires and fireballs. The radiative fraction is strongly dependent on the soot content and temperature of the flame, but measurements above 0.4 are rare. The rational and origin of the relationship are unclear, but it has been adopted by OGP [10], and therefore it is significant to show that it results in overprediction in this case. Equation (8) is an empirical relationship with no link to the physics of the phenomena. Interestingly Wang and Co-workers [8] used the same expression giving Fr = 0.7, in their case. They also showed good agreement with their data from LNG experiments, which will have different sooting characteristics to the current case. Additionally, a low heat of combustion was used in Wang et al [8], without explanation.

As a comparison Eq. (8) in the above model was replaced with Fr = 0.3 (i.e. the generic value typically used radiative fire hazard calculations). The results are shown as a dashed line in Fig. 5, and clearly demonstrate a much better agreement with the experimental test data from this work.

Worthy of note is the result from Eq. (3), with a duration of the fireball from this release of 17.4 s, which compares well with the duration of the thermal pulse indicated in Fig.3.

Thermal damage to vegetation

During the second test, two types of plants (Laurustinus and Portuguese Laurel) were located at each of the radiometer locations. During the second test the leaves of the Portuguese Laurel at 200 m showed scorching (shown in Fig. 6). However, grass located 150 to 250 m from the release point was ignited.

In fire hazard calculations the minimum heat flux required either for pilot ignition or autoignition of solid material is a very important parameter, as it defines the ignition propensity of the material. As it is the minimum heat flux that is of interest then necessarily the exposure times are long. For example for wood the minimum heat flux required to achieve piloted ignition, is typically quoted as 12.5 kW/m^2,while for autoignition it is 29 kW/m^2 [11]. However, it should be understood that at these heat fluxes it may take several minutes before ignition occurs.

The exposure time to fireballs resulting from pipeline ruptures, or other transient events, is short but the actual incident heat fluxes are large. For this reason, the minimum heat flux data for pilot ignition or autoignition of the material is of little use in establishing the thermal threat level that these events pose to their surroundings. More work is needed in this area to develop a database of ignition propensity to short high intensity heat fluxes.

With respect to the second test, it is possible that hot embers and debris could have fallen onto the grass to cause piloted ignition in patches, as shown in the debris field in Fig. 7. However, it is also likely that the radiative flux was sufficient to ignite the grass in June when most likely it was dryer than in March.

There are many variables which will affect whether vegetation will ignite: Type of solid (thermally thin or thick), ambient conditions, size and orientation of object, heating methods, moisture levels, fuel arrangement, topography. Also, different species will have varying resistance to fire, for example juniper trees have a thin bark and a lack of other defence mechanisms, so will be sensitive to fires [12].

Moisture levels are an important variable for vegetation, as a substance needs to be dry for combustion. to occur and, as water has a high latent heat of vaporisation, considerable thermal radiation is needed to dry out a substance [13].

Fig. 6. Scorching to Portuguese Laurel – Test-2, 200 m.

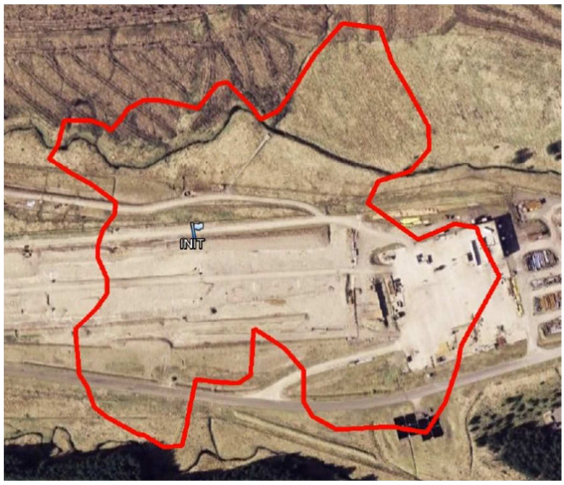

Fig. 7. Debris field.

Ignition of cellulosic materials determined in the laboratory is likely to have been conducted on substances which have been dried out. However, as shown in the second test, the intensity of radiation from the fireball phase is sufficient to dry out a substance and cause combustion to occur.

Weather conditions also play a role, as a long dry period, will make the ecosystem easier to ignite. Damage to grass was limited in the first test, which is likely to be due to significant rain and snow in advance of the test.

In the event of a real release, the fireball phase will be followed by a steady state fire. The duration of this steady state fire will be dependent upon how easily the plant is to isolate. In 2004, an 80 bar, 40-inch gas pipeline ruptured [14]. Thermal damage was caused, extending to a radius of approximately 200 m which is equivalent to 125,000 m^2. Figs. 8 to 10 show damage to trees, grass and timber pallets around the building.

In the UK, environmental risk assessments can be carried in line with the Chemical and Downstream Oil Industries Forum (CDOIF) guidance on environmental risk tolerability [15].

To determine whether there is the potential for a major accident to the environment (MATTE) the following steps can be carried out:

1. Deduce credible scenarios to assess;
2. Determine whether there is pathway to cause harm to a receptor (i.e. thermal radiation);
3. Calculate the hazard distance to determine which receptors would be affected;
4. Assess the area of damage caused for different receptors against the CDOIF guidance;
5. Determine the duration of the harm.

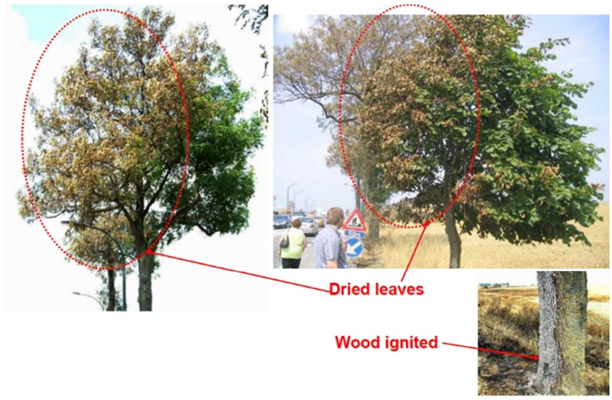

Fig. 8. Damage to trees 210 m from the crater [14].

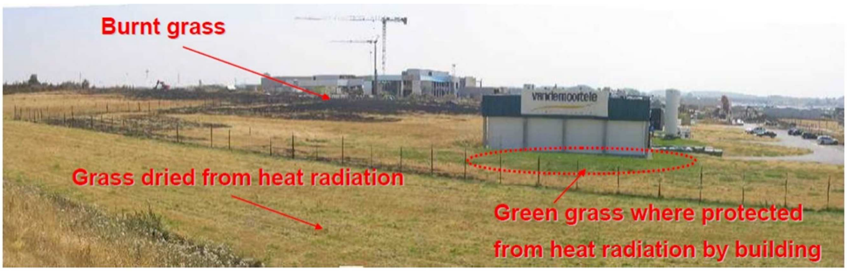

Fig. 9. Damage to grass. View 400 m from the crater [14].

Fig. 10. Damage caused to wooden pallets 130 m from the crater [14].

In the case of a pipeline rupture, Figs. 8 to 10 show that harm can be caused by a pipeline rupture to environmental receptors. Area criteria for assessing damage to environmental receptors start from 0.5 hectares (5,000 m^2) or 10% of the area, if less for sensitive receptors and 10 hectares (100,000 m^2). The experimental data have shown that in the initial fireball phase of a pipeline rupture, visible damage to vegetation is caused to plants within 200 m of the release. Most of the burnt area in this case was grass. Grass has an unusual growth mechanism in that it starts from the stem, rather than the tip [13]. Therefore, unless the soil is badly damaged it is likely for the grass to re-grow. In assessing the possible impacts for grass, it is likely to recover within 3 years and so therefore, it is in accordance with the CDOIF guidelines, such an incident would not be classed as a MATTE.

Other criteria are included with the CDOIF guidelines and further information is required in assessing the consequences more sensitive receptors.

CONCLUSIONS

Two large scale tests of fireballs from full-scale, below-ground, natural-gas pipeline rupture enabled experimental measurements of the thermal radiation levels generated to be made. The duration of the fireball and the maximum heat fluxes were well predicted by current simple mathematical models when a reasonable radiative fraction of the total energy release is assumed. The empirical radiant fraction equation adopted by OGP was shown to overpredict the incident heat flux. In the second test the grass surrounding the test location was ignited and other vegetation showed significant thermal damage. To interpret such data correctly and to evaluate the hazards presented by such pipeline ruptures to natural and man-made environments more information is needed on the effects of short exposure times of the order of a few seconds to high transient heat fluxes.

REFERENCES

[1] Energy Transition Outlook 2018 Oil And Gas, Forecast to 2050, DNV GL, 2018.

[2] Incident Statistics. PHMSA. https://www.phmsa.dot.gov/hazmat-program-management-data-and-statistics/data-operations/incident-statistics, 2018 (accessed 11 May 2018).

[3] Gas Pipeline Incidents, 9th Report of the European Gas Pipeline Incident Data Group 1970-2013, EGIG 14.R.0403, 2015.

[4] R.P. Cleaver, P.S. Cumber, P. Genillon, A Model to Predict the Characteristics of Fires Following the Rupture of Natural Gas Transmission Pipelines, Process Saf. Env. Prot. 79 (2001) 3–12.

[5] R.P. Cleaver, A.R. Halford, A model for the initial stages following the rupture of a natural gas transmission pipeline, Process Saf. Env. Prot. 95 (2015) 202–214.

[6] B.J. Lowesmith, G. Hankinson, M.R. Acton, G. Chamberlain, An Overview of the Nature of Hydrocarbon Jet Fire Hazards in the Oil and Gas Industry and a Simplified Approach to Assessing the Hazards, Process Saf. Env. Prot. 85 (2007) 207–220.

[7] S. Mannan (Ed.), Lees' Loss Prevention in the Process Industries (Fourth Edition), Vol. 1, Ch. 16: Fire, pp. 1075-1366, Elsevier, 2012.

[8] K. Wang, Z. Liu, X. Qian, P. Huang, Long-term consequence and vulnerability assessment of thermal radiation hazard from LNG explosive fireball in open space based on full-scale experiment and PHAST, J. Loss Prev. Process Ind. 46 (2017) 13–22.

[9] M.R. Acton, G. Hankinson, B.P. Ashworth, M. Sanai, J.D. Colton, A Full Scale Experimental Study of Fires Following the Rupture of Natural Gas Transmission Pipelines, p. V001T01A008, 2000.

[10] Consequence Modelling, OGP, 434–07, 2010.

[11] D. Drysdale, An introduction to fire dynamics, 3rd ed, Chichester, Wiley, 2011.

[12] P. Evangelista, T. Stohlgren, D. Guenther, S. Stewart, Vegetation Response To Fire And Postburn Seeding Treatments In Juniper Woodlands Of The Grand Staircase-Escalante National Monument, Utah., Western North American Naturalist 64(3) (2004) 13.

[13] Effect of Fire on Vegetation, R2842, DNV GL, 1999.

[14] Rupture and ignition of a gas pipeline, ARIA, 2009.

[15] Environmental Risk Tolerability for COMAH Establishments, Chemical and Downstream Oil Industries Forum, Version 2.